The Next Generation Integrity Monitor Testbed (IMT) for Ground System Development and Validation Testing

Per-Ludvig Normark, Gang Xie, Dennis Akos, Sam Pullen, Ming Luo, Jiyun Lee, and Per Enge
Department of Aeronautics and Astronautics, Stanford University

Boris Pervan
Department of Mechanical, Materials, and Aerospace Engineering, Illinois Institute of Technology

ABSTRACT

The Stanford University Integrity Monitor Testbed (IMT) is a prototype of the Local Area Augmentation System (LAAS) Ground Facility (LGF). It is used to evaluate whether the LGF can meet the integrity and continuity requirements that apply to Category I precision approach. With support from the U.S. Federal Aviation Administration (FAA), Stanford University has developed IMT algorithms and has implemented them in real-time with special emphasis on automated fault diagnosis and recovery. The first generation IMT hardware was designed in the mid-1990s, and since then computer power and receiver technology has evolved significantly. Therefore, a transition has been made to a new and improved system to further development and testing for Category I precision approach and to use as a starting point for Category II/III LGF development.

This paper describes the hardware and motivation behind the second-generation IMT system. One key element of the upgrade has been the development of new software to communicate with the receivers. This function, known as Signal-in-Space Receive and Decode (SISRAD), is now a modular means of integrating different receiver types, providing synchronization of receiver measurement packets, and extracting receiver measurement packets into a specified IMT data format.

With these modifications, the new IMT is able to support more extensive and efficient nominal and failure testing. The upgrade has been completed, and in this paper present nominal data fault free data is presented along with how the IMT responds to a satellite clock ramp failure.

1.0 INTRODUCTION

The U.S. Federal Aviation Administration (FAA) is developing the Local Area Augmentation System (LAAS) to support aircraft precision approach. The LAAS architecture (Figure 1) consists of three components:

I. The space segment (GPS)
II. The user (aircraft)
III. The Local Ground Facility (LGF)

This local-area differential GPS ground-based system places the responsibility for detecting and alarming space-segment and ground-segment failures on the LAAS Ground Facility (LGF), which is also responsible for generating and broadcasting carrier-smoothed code differential corrections and approach-path information to user aircraft [1]. The LGF must insure that all ranging sources for which LAAS corrections are broadcast are safe to use. If a failure occurs that threatens user safety, the LGF must detect and alert users (by not broadcasting corrections for the affected ranging source) within 3 seconds. Category I precision approaches have a 6 seconds time-to-alarm and the LGF has three of those seconds while the user is allocated the other three seconds.

The LGF must apply several different types of monitoring algorithms to detect a varied array of possible failures. In order to coordinate the LGF response to detected failures (some of which may trigger more than one monitoring algorithm), complex failure-handling logic must be included in the LGF. Stanford University researchers have developed an LGF prototype known as the Integrity Monitor Testbed (IMT) that includes a comprehensive set of monitoring algorithms and Executive Monitoring (EXM) logic to isolate failed measurements and reintroduce these measurements after the failure is clearly determined to be over.

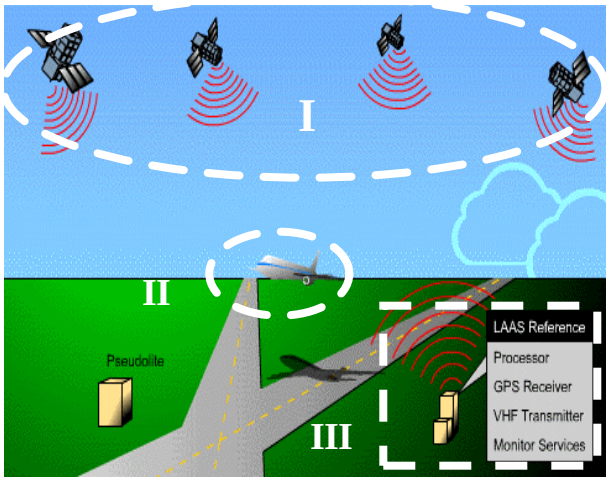

Figure 1 LAAS Architecture

In order to show that the requirements in the LGF Specification are achievable, it is important to verify that the IMT works as designed and meets the LGF integrity requirements. The most frequently used method for testing different ranging source failures is to inject failures in software by modifying stored IMT reference receiver packets (from measurements taken under nominal conditions) and let the IMT post-process the altered measurements.

This paper gives an overall picture of the IMT system architecture and hardware. It briefly explains integrity monitor algorithm components and shows nominal fault free data. The new Signal-in-Space Receive and Decode (SISRAD) component is explained in detail. Finally, the plans for the next phase of IMT development and testing are discussed. Note that an updated version of the LGF Specification for Non-Federal procurement was released [11] earlier this year. The IMT is designed to satisfy the more specific integrity requirements of the previous specification and, with minor exceptions (several new algorithms are now being implemented for such exceptions) it meets the revised specification as well.

2.0 IMT HARDWARE COMPONENTS

The IMT system (Figure 2) consists of three GPS antennas, three GPS L1 receivers and a PC workstation that processes the 2 Hz GPS measurements.

ANTENNAS

The three antennas are NovAtel L1/L2 Pinwheel 600 active antennas. These are designed to minimize multipath and they have performance comparable to a choke ring, but are smaller in size. These are placed at surveyed locations at the Hansen Experimental Physics Laboratory (HEPL) roof at Stanford University, separated sufficently to keep any resulting multipath uncorrelated [5].

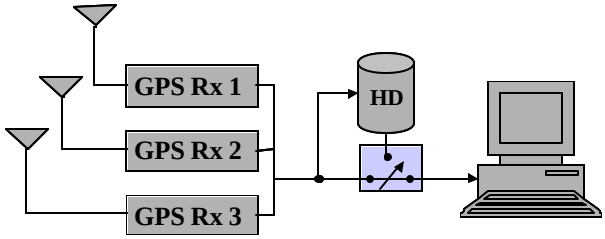

Figure 2 IMT hardware components

ANTENNA CABLES

The cables between the antennas and the receivers are of good quality (Belden 9913, RG/U-8) and the length ranges from 50 to 100 meter. The length introduces losses in the signal and the measured losses for each antenna can be found in Table 1. The loss in each cable was measured using a signal generator connected to one end producing a sinusoid at 1600 MHz (GPS L1 frequency is at 1575.42 MHz) at 0 dBm power and a power meter connected to the other end.

Antenna	Loss (in dB)
Rx1	-13.5 dB
Rx2	-15.9 dB
Rx3	-11.6dB

Table 1 Antenna cable losses

These signal losses have to be considered in regard to the resulting receiver noise figure and automatic gain control. As a result thresholds for the Signal Power Test (see section 4) have to be individually selected for each reference receiver. A better solution may be to place the GPS receiver next to the antenna and use a low latency digital channel to transfer the GPS measurements to the computer. Unfortunately this is not a practical solution for the current IMT configuration, but as long as the signal losses are known, they can be accounted for and will not produce any problems for the test and development.

GPS RECEIVERS

The GPS receivers are NovAtel OEM4 RT-20 (L1 C/A code only). If needed, these can be upgraded (by firmware) to also use the L2 frequency.

PC WORKSTATION

The PC used is a dual Pentium Xeon 400 MHz computer equipped with a PCI multi port serial card that adds eight extra serial COM ports (Comtrol Rockport PCI card). The main focus of the choice of PC platform is to provide a relatively fast and flexible develop environment. The operating system chosen was Red Hat Linux 7.1, which is

a multi user system that provides a robust and stable environment.

3.0 IMT SYSTEM ARCHITECTURE

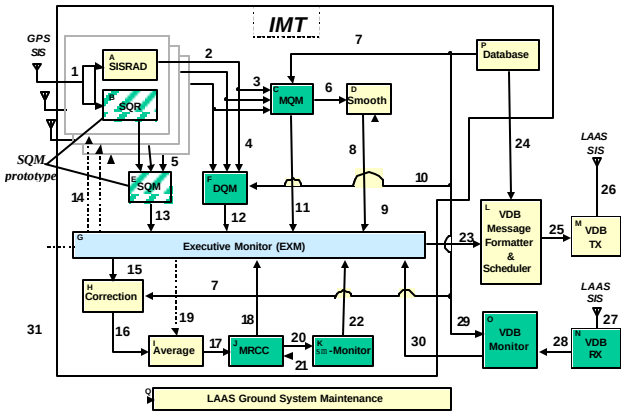

Figure 3 IMT Functional Block Diagram

Figure 3 shows the functional system architecture of the IMT as currently implemented. Boxes inside the solid line are components of the Stanford IMT (everything except the VHF Data Broadcast (VDB) up/downlink), boxes marked with dashed green (Signal Quality Receiver (SQR), Signal Quality Monitor (SQM)) are implemented as separate test prototypes and currently not integrated into the IMT [10].The IMT functions can be divided into three groupings [4]:

a) *Nominal Differential GPS Operations* (white boxes in Figure 3). These comprise the nominal tasks of a differential system: decode the GPS signals, carrier smooth the pseudorange, generate pseudorange corrections and average the measurements and broadcast the results to the user.

b) *Integrity Monitor Algorithms* (green boxes in Figure 3). Together with c) this is the major focus for Stanford University on the developing LGF. The LGF integrity monitor algorithms are targeted at a wide range of possible failures in the GPS SIS or in the LGF itself and are designed to insure that threatening failures are detected within three seconds at least 99.9% of the time. Each algorithm generates one binary flag (failure/ok) per channel (a given satellite tracked on a given receiver) or per satellite. In this paper, nominal data from a subset of the monitors are presented, but the monitors are not described in detail, refer to [3,7,9,13] for details.

c) *Executive Monitoring (EXM)* (light blue boxes in Figure 3). These are the logic functions that combines the results of the integrity monitors and takes the appropriate action. If a single flags occurs on a single receiver, the measurement is excluded, if several channels flag on a single receiver, the receiver is excluded and if the same satellite fails on a more then one receiver, the satellite is excluded. For a detailed description of this logic, refer to [3].

3.0 SISRAD

Signal-in-Space Receive and Decode provides the LGF with GPS L1 signal measurements at a 2 Hz rate (pseudorange, carrier-phase, C/No) and satellite navigation data (ephemeris and almanac) for each reference receiver.

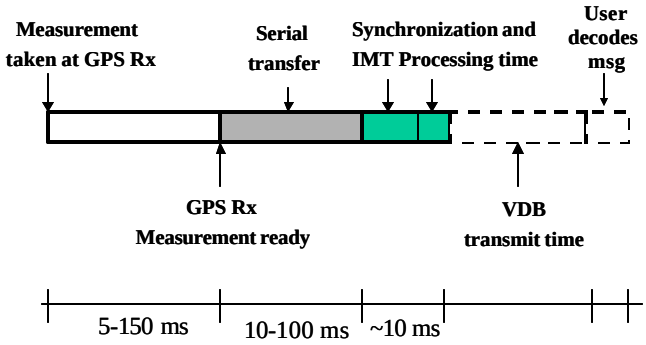

Figure 4 GPS Measurement time-to-algorithms

Most high quality GPS receivers operate as stand-alone equipment with a serial asynchronous communication link (RS-232, RS-422) to transfer measurements to other equipment (in this case the IMT computer). All messages are formatted in a receiver specific format and time-tagged with GPS time. These messages are transferred over the serial link for further processing in IMT computer. Referring to Figure 4, there is a non-deterministic time that elapses from when a GPS measurement was actually taken until it is ready for processing in the IMT computer. First, there is an internal delay in the GPS receiver (receiver specific, cannot be controlled by the user), then there is a serial transfer delay (can be minimized by using a high baud rate) and finally there is a decode time of the message in the computer. In the IMT, GPS measurements are received at a 2 Hz rate and the serial transfer baud rate used is 115200 bps (bits-per-second).

Figure 5 plots the difference of the GPS time (t_{GPS}) and computer arrival time (t_{PC}) where the computer arrival time is defined as the computer system time when the message was decoded in the computer. The data plotted is over is a 6 hour period with range measurements (pseudorange, carrier-phase etc.) delivered every 0.5 seconds, ephemeris data delivered every 30 seconds, and almanac (delivered every 750 seconds).

$$A_0 = t_{GPS}(0) - t_{PC}(0) \quad (1)$$

$$diff(k) = t_{GPS}(k) - t_{PC}(k) - A_0 \quad (2)$$

$$drift_{PC}(k) = A_0 + a * k \quad (3)$$

$$diff'(k) = t_{GPS}(k) - t_{PC}(k) - drift_{PC}(k) \quad (4)$$

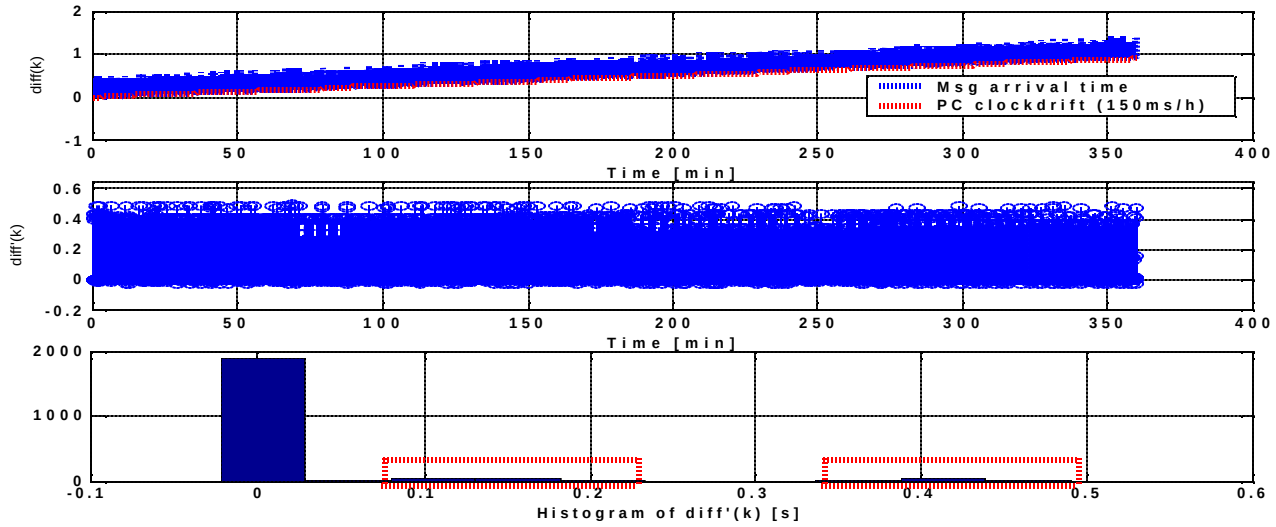

Figure 5 Variance of GPS message delivery time

In the top plot of Figure 5 (Equation 1) the computer clock drift is clearly shown. If the data is fit to a line, the computer clock drift (denoted a) can be determined, and in this case a is about +150 ms/hour . The second plot in Figure 5 plots diff'(k), (Equation 4, computer clock drift removed) and here the variance of the measurements is shown (bin size 0.05 seconds). A histogram of the same data (Equation 4) is shown in plot 3 of Figure 5. Three distinct "bins" can be distinguished. The first bin shows that most of the messages are delivered within 50 ms, the second "bin" (150 ms) shows the internal GPS receiver delay for the range message (the range message delay can be from 5-150 ms according to NovAtel documentation) and the last "bin" shows when the ephemeris and almanac messages are delivered (the bandwidth of the serial link and receiver processing delays the delivery).

The SISRAD module is designed together with a IMT message format to be able to interface different GPS receivers (Figure 6).

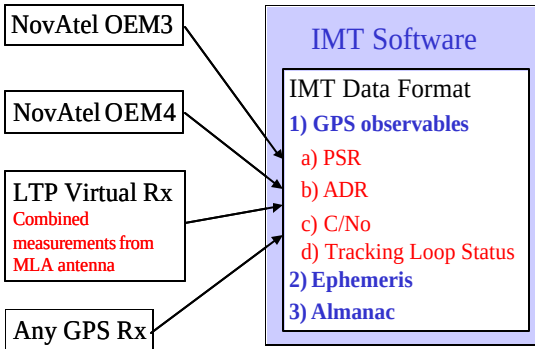

Figure 6 Different GPS Rx formats

Three different IMT messages are defined: (1) range message which consists of: a) pseudorange, b) carrier-phase, c) C/No, and d) tracking loop status; (2) ephemeris, and (3) almanac. One of the motivations behind this design approach was to be able to post process the FAA's LAAS Test Prototype (LTP) data files. The LTP uses a special type of Multipath Limiting Antenna (MLA) [14]. Figure 7 shows a cartoon of the antenna. It consists of one helibowl antenna that receives high elevation satellite signals and one dipole antenna that receives low elevation satellite signals. Each antenna component is connected to a NovAtel OEM3 receiver and measurements are combined in software to a single "virtual receiver" measurement (pseudorange and carrier-phase from the two receivers are combined and phase calibrated).

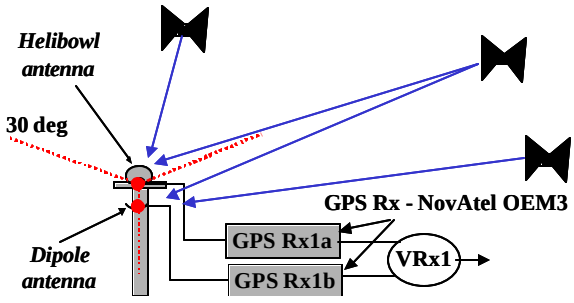

Figure 7 Multipath Limiting Antenna – MLA

The FAA Technical Center does the combination of the two receivers and can provide "virtual receiver " data. It is important to verify that the IMT works with this type of antenna as it is expected that the MLA will be integral part of a future LAAS system.

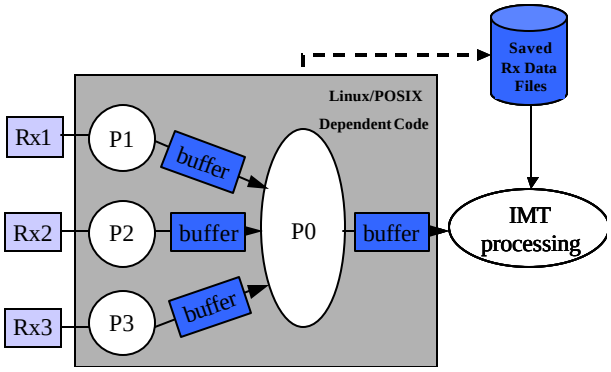

Figure 8 SISRAD Software Process Hierarchy

The design of the SISRAD software is illustrated in Figure 8. Each GPS receiver is represented by a software process (P_1, P_2, P_3) that reads the GPS receiver specific format from the serial port and re-packs the message into the IMT format and then delivers the message through a buffer to the synchronization process (P_0). The synch process looks at the GPS time of each message and ensures that every message from epoch *k* is delivered before any message from epoch *k+1* are delivered to the IMT process.

4.0 NOMINAL DATA

Nominal data from the new IMT system is presented next. The dataset is from 20 June 2001 (LAAS laboratory, Stanford University). Each plot is briefly explained and for a detailed description of the integrity algorithms, refer to [3]

The purpose of the Signal Quality Monitor is to ensure that that no presence of C/A signal-deformation *evil waveforms* [6] exists. To perform this test, a modified reference receiver is needed (SQR, multicorrelator receiver [10]). This SQM prototype is being failure tested separately and is currently not integrated in the IMT. SQM also has a separate algorithm to ensure that the received satellite signal power is within SPS specifications and this monitor is implemented in the IMT. The signal-power monitor (Figure 9) takes an average of reported receiver C/N_0 for each channel at the current epoch *k* and the value at the previous epoch (*k*-1):

$$C/N_{o\_Avg}(k) = \frac{1}{2}\left(C/N_o(k-1) + C/N_o(k)\right) \quad (5)$$

The averaged C/N_0 is compared with a threshold value. The threshold is elevation angle dependent (highly dependent on the antenna gain pattern) and nominal test data provides the basis for the threshold calculation.

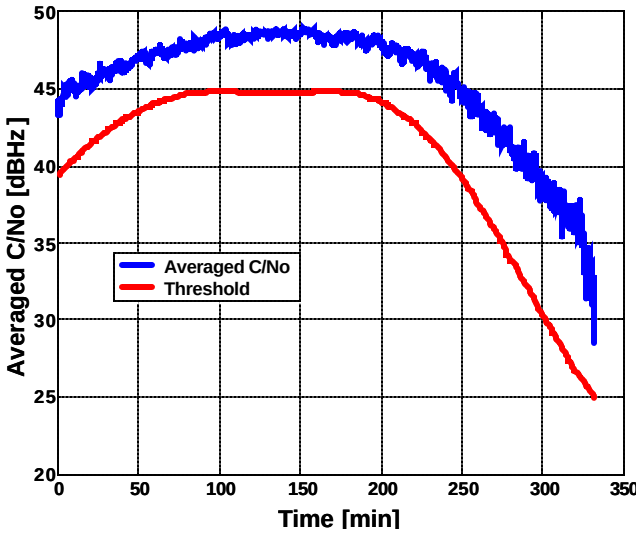

Figure 9 Signal Power Test Rx1-Prn8

Under nominal conditions measurement means and standard deviations are calculated in each bin with 10° difference of elevation, i.e., 0°-10°, 10°-20°,…, 80°-90°. These 9 points of means and 9 points of standard deviations are used to calculate 9 points of thresholds, i.e., C/No threshold = μ-6*σ

$$C/N_{o\_Threshold}(k) = m - 6 * s \quad (6)$$

In the current IMT, a 4th-order polynomial curve is used to interpolate thresholds at other elevation values.

Measurement Quality Monitor (MQM) confirms consistency of pseudorange and carrier-phase measurements over the last epochs to detect rapid changes (steps, ramps) dues to satellite clock anomalies. MQM includes three monitors that are combined into a single flag (by logically "or"-ing the outcome of the MQM monitors). The carrier-step acceleration test (Figure 10) is designed to detect rapid changes in the carrier-phase measurement that could cause errors in the pseudorange corrections. On a given reference receiver the last 10 epochs (5 seconds of data, 2 Hz update rate) of carrier-phase measurements is fit to a quadratic model [3].

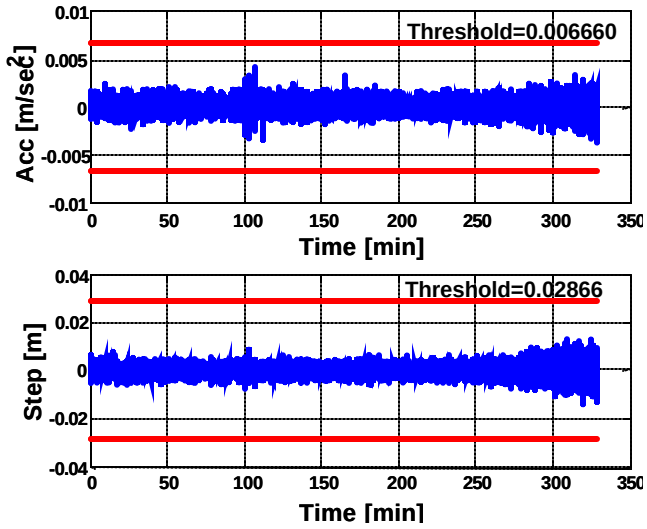

Figure 10 Step-Acceleration Test (Rx1-Prn8)

Based on theoretical analysis and nominal testing, acceleration and step thresholds, with SA on, are set to be seven times their standard deviations in order to limit the probability of flags under fault-free conditions to levels low enough to meet the LGF continuity requirements [1,2].

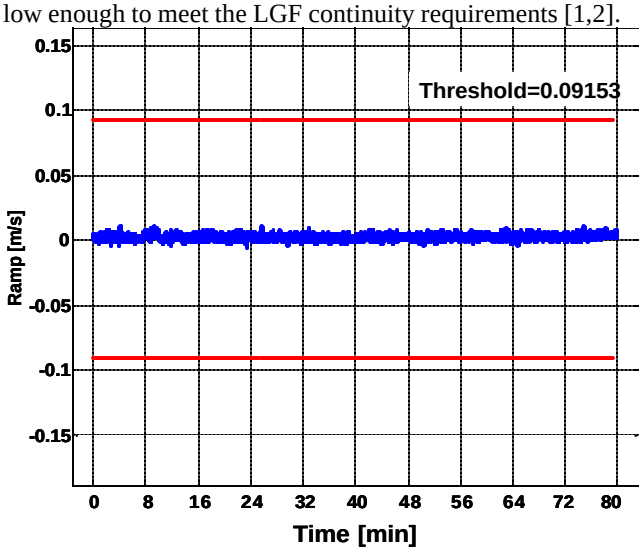

Figure 11 MQM Ramp Test (Rx1-Prn8)

The MQM Ramp test (Figure 11) has been recently added to the IMT. The first order coefficient is monitored to ensure that the carrier-phase measurement does not linearly increase or decrease out of specification.

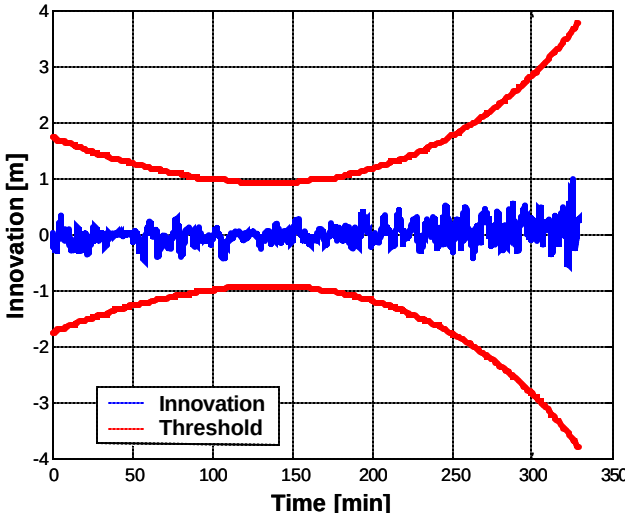

Figure 12 Innovation Test (Rx1-Prn8)

The carrier smoothed code innovation test is designed to detect rapid changes on the raw pseudorange measurement (i.e impulse and step errors). In order to limit fault-free alarms, the innovation elevation dependent threshold is set as 6.82 times its theoretical standard deviation [3].

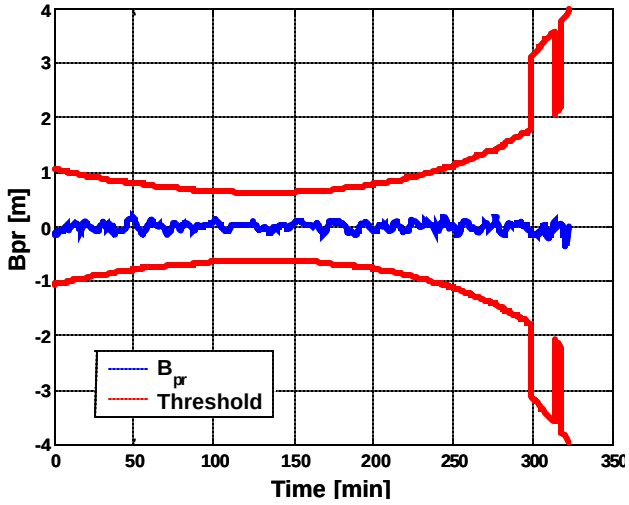

Figure 13 MRCC B-Value Test (Rx1-Prn8)

Multiple Receiver Consistency Check (MRCC) expresses the consistency of the corrections produced for each satellite across all reference receivers. B-values [3] are computed and compared to an elevation angle dependent threshold. B-values are needed as they are broadcast to users (they are needed for users to compute "H1" protection levels) and to isolate any receivers or receiver channels that create anomalously large errors in the corrections.

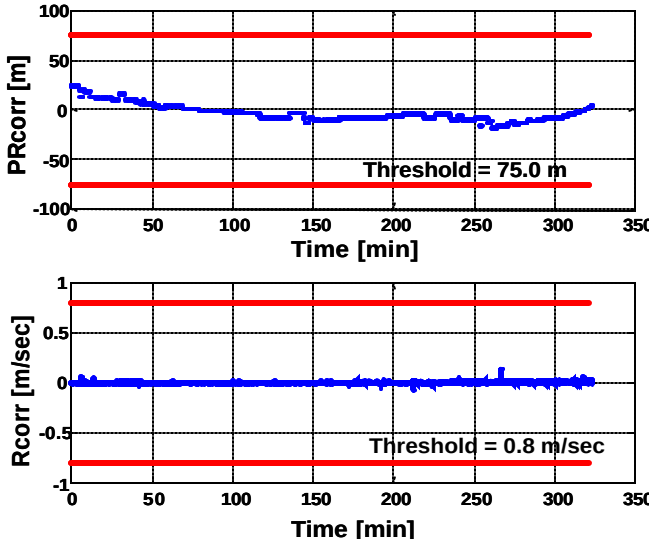

Figure 14 MFRT Correction Generation Test (PRN 8)

Message Field Range Test (MFRT) is the last monitor before measurements are approved for broadcast. It ensures that the calculated corrections are less then ±75 m (SA off, ±327 m with SA on) and the rate of the correction is less the ±0.8 m/s (SA off, ±3.4 m/s SA on).

5.0 SATELLITE CLOCK FAILURE

It is very important to verify that the IMT can detect all possible failure modes. When a real-world failure occurs, it becomes a new "failure-mode" that has to be protected. In the IMT, different failures are simulated by modifying stored nominal data and then that data is re-run through the IMT to verify that the IMT behaves as expected. In this specific failure test, we show that the IMT can immediately detect a large satellite clock drift. The nominal stored data from 20 July 2001 is modified to simulate a satellite clock ramp drift of 2.5 m/s. This failure is similar to what happened with PRN 22 on 28 July 2001. The PRN 22 clock started ramping with a drift rate of 2.5 m/s to 5 m/s. This introduced large pseudorange errors (1900 meters after 10 min) [15]. A clock ramp is not hazardous to a LAAS user since the LGF can correct for the error, but once the satellite clock has failed, it cannot be predicted what will happen next, and the satellite should be excluded.

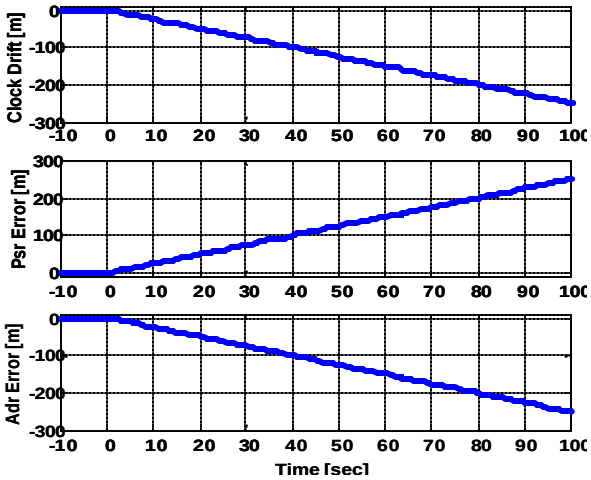

Figure 15 Satellite clock ramp failure

Figure 15 shows how the clock drift affects both the pseudorange and the carrier-phase. The convention of the sign of pseudorange and carrier-phase in the GPS receiver used in the IMT makes an increase of the pseudorange a decrease of the carrier-phase. At time 0 the satellite clock drift is inserted into the pseudorange and carrier-phase.

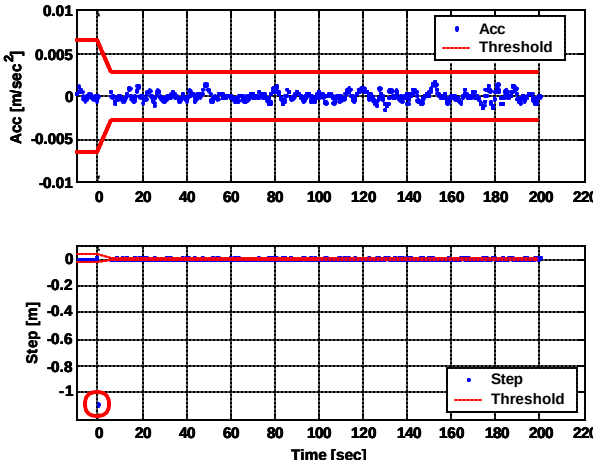

Figure 16 MQM Step-Acceleration test

In the first epoch after the satellite clock drift is inserted, the MQM step test flags the failure (plot two, Figure 16). The quadratic carrier-phase model is restarted, and the next test point occurs 10 epochs later. When the next test point is ready, the MQM step test does not flag the failure again but the MQM ramp test flags it (Figure 17) since the linear drift of the carrier phase is exceeding its threshold.

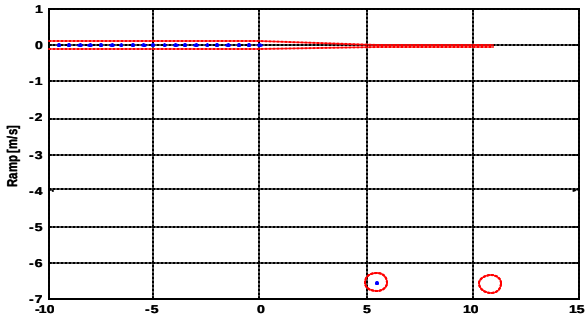

Figure 17 MQM Ramp test

If the MQM ramp test would not flag the failure (i.e if the clock drift is so small that it will pass the MQM ramp threshold) and if no other monitor (now using a reduced threshold since the MQM step has flagged once) would flag the failure, the satellite would be introduced after 200 seconds.

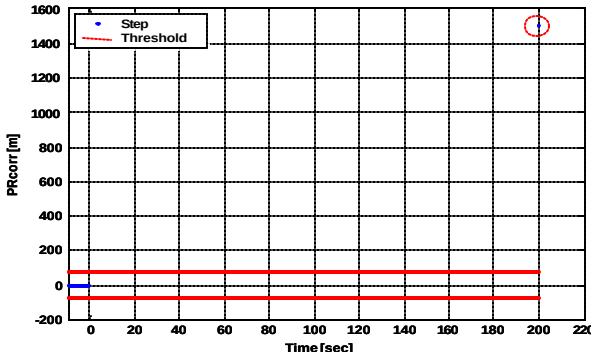

Figure 18 MFRT test

If this would happen, as shown in Figure 18, the MFRT test would catch the failure (correction magnitude for the satellite is 1500 m and the maximum correction with SA off is ±75 m) and exclude the satellite for the entire pass.

6.0 CONCLUSIONS AND FUTURE WORK

This paper has discussed the new hardware and the SISRAD software of Stanford's LAAS Integrity Monitor Testbed (IMT) in detail. The new IMT system consists of up to date hardware and provides a more flexible development environment. It can also be used as starting point for Category II/III algorithm development. Nominal fault free data is presented along with data with a simulated satellite clock ramp failure (similar to what happened with PRN 22 on 28 July 2001). The results show the ability of the IMT to immediately detect and isolate such failures. During the fall, testing the IMT with LTP data will be performed and the user interface to the IMT will be improved to take advantage of the new platform. These two tasks will be done in parallel with IMT algorithm development and further failure testing.

ACKNOWLEDGEMENTS

The authors would like to give thanks to many other people in the Stanford GPS research group for their advice and interest. Funding support from the FAA Satellite Navigation LAAS Program Office (AND-710) is appreciated. The opinions discussed here are those of the authors and do not necessarily represent those of the FAA and other affiliated agencies.

REFERENCES

[1] *Specification: Performance Type One Local Area Augmentation System Ground Facility*. U.S. Federal Aviation Administration, Washington, D.C., FAA-E-2937, Sept. 21, 1999. Internet: http://gps.faa.gov/Library/Documents/laas_faa2937.pdf

[2] "FAA LAAS Ground Facility (LGF) Functions," Version 2.4. LAAS KTA Group, Unpublished Manuscript, September 9, 1998.

[3] G. Xie, S. Pullen, *et.al*., "Integrity Design and Updated Test Results for the Stanford LAAS Integrity Monitor Testbed,", ION 57th Annual Meeting, Albuquerque, NM, June 11-13, 2001, pp. 681-693.

[4] S. Pullen, M. Luo, *et.al*., "GBAS Validation Methodology and Test Results from the Stanford LAAS Integrity Monitor Testbed,", *ION GPS 2000*, 19-22 September 2000, Salt Lake City, UT, pp. 1191-1201.

[5] M. Luo, S. Pullen, "LA AS Reference Receiver Correlation Analysis," Stanford University, Unpublished Manuscript, Feb. 17, 1999.

[6] D. Akos, *et.al*., "GPS Signal Quality Monitoring: Test Results," *Proc. of the ION 2000 National Technical Meeting*. Anaheim, CA., Jan. 26-28, 2000, pp. 536-541.

[7] S. Pullen, *et.al*., "The Use of CUSUMs to Validate Protection Level Overbounds for Ground-Based and Space-Based Augmentation Systems," *Proceedings of ISPA 2000*. Munich, Germany, July 18-20, 2000.

[8] B. Pervan, *et.al*., "Sigma Estimation, Inflation, and Monitoring in the LAAS Ground System," *Proceedings of ION GPS 2000*. Salt Lake City, UT., Sept. 19-22, 2000, pp. 1234-1244.

[9] J. Lee, S. Pullen, *et.al*., "LAAS Sigma Monitor Analysis and Failure-Test Verification,", ION 57th Annual Meeting, Albuquerque, NM, June 11-13, 2001, pp. 694-704.

[10] A. Mitelman, *et.al*., "A Real Time Signal Quality Monitor for GPS Augmentation Systems," *Proceedings of ION GPS 2000*. Salt Lake City, UT., Sept. 19-22, 2000, pp. 862-871.

[11] *Specification: Category I Local Area Augmentation System Non-Federal Ground Facility*. U.S. Federal Aviation Administration, Washington, D.C., FAA/AND710-2937, May 31, 2001.

[12] F. van Graas, "Detection of Satellite Low Signal Power." Ohio University, Revised Draft, April 30, 2001.

[13] S. Pullen, M. Luo, B. Pervan, F.C. Chang, "Ephemeris Protection Level Equations and Monitor Algorithms for GBAS," *Proceedings of ION GPS 2001*. Salt Lake City, UT., Sept. 11-14, 2001.

[14] R. Braff, "Description of the FAA's Local Area Augmentation System (LAAS)," Navigation. Vol. 44, No. 4, Winter 1997-1998, pp. 411-424

[15] S. Pullen et.al, A Quick Look at Last Weekend's SVN/PRN 22 Clock Anomaly", Stanford University, Aug. 3, 2001.